

# Large Eddy simulations and Reynolds-averaged Navier-Stokes simulations of separation-induced transition using an unstructured finite volume solver

Manuel Carreño Ruiz<sup>1,a</sup> \* and Domenic D'Ambrosio<sup>1,b</sup>

<sup>1</sup> Department of Mechanical and Aerospace Engineering, Politecnico di Torino, C.so Duca degli Abruzzi, 24, 10124 Torino, Italy

<sup>a</sup>manuel.carreno@polito.it and <sup>b</sup>domenic.dambrosio@polito.it

**Keywords:** Laminar Separation Bubbles (LSB), Large Eddy Simulation (LES), Transition Modelling, Reynolds Averaged Navier Stokes (RANS)

**Abstract.** The study aims to assess the capability of different methodologies in capturing the separation-induced transition phenomenon. This transition mechanism occurs when the flow separates from the airfoil surface, and transitions from a laminar to a turbulent state due to the amplification of the Kelvin-Helmholtz instability developed in the separated shear layer. The simulations employ high-order numerical methods for solving the Navier-Stokes equations, while the transition modeling for RANS is based on the  $\gamma - Re_\theta$  transition model. LES enables prediction of the onset and location of transition and provides turbulent flow statistics.

## Introduction

Predicting flow transition on airfoils is crucial for designing unmanned aerial systems, as it directly impacts their aerodynamic performance, stability, and control. However, accurately predicting flow transition remains challenging due to the complex nature of flow physics and the limited availability of high-fidelity experimental data, especially in the very-low Reynolds number regime. One extensively studied benchmark case in this regard is the SD7003 airfoil. Galbraith et al. [1] carried out Implicit Large Eddy Simulations (ILES) using a Discontinuous Galerkin method to study flow transition on the SD7003 airfoil. Uranga et al. [2] corroborated the good performance of ILES in computing separation-induced transition, testing Reynolds numbers as low as 22,000. Catalano et al. [3] presented LES results using a second-order scheme for the chordwise and wall-normal directions, employing Fourier collocations in the spanwise direction. They contested the conclusions of [1], which claimed the necessity of a high-order scheme to capture laminar separation bubbles. In fact, second-order schemes can adequately capture separation-induced transition, albeit with extremely refined grids. RANS approaches have also been employed for studying the SD7003 airfoil. Windte et al. [4] coupled a  $k-\omega$  model with an  $e^N$  transition model to predict transition around the airfoil. Catalano et al. [5,6] proposed modifications to the  $k-\omega$  SST turbulence model to better capture lower Reynolds number flows, applying it to this specific airfoil. De Santis et al. [7] recently introduced a modification of the  $\gamma$  transition model [8] to enhance turbulent kinetic energy production within separation bubbles. Carreño et al. [9] also attempted to increase turbulent kinetic energy production in separation bubbles by tuning the  $s_1$  parameter in the  $\gamma - Re_\theta$  transition model [10].

This study uses LES to predict flow transition on the SD7003 airfoil at Reynolds number 60,000 and Mach number of 0.2. We examine different numerical settings for LES, focusing on the impact of selecting higher-order and less dissipative schemes. We compare the velocity field created by the separation bubble using the RANS model described earlier and LES. Additionally, we present a comparison between the WALE and dynamic Smagorinsky subgrid-scale models.

## Numerical Methods

Numerical simulations in this paper were conducted using the commercial software STAR-CCM+. The SD7003 airfoil geometry at an angle of attack of 4 degrees was employed for this analysis. To minimize the influence of the far-field boundary, the computational domain was extended to approximately 100 chords. The RANS equations were solved on a two-dimensional grid. A time-accurate implicit second-order integration was utilized to capture the vortex shedding that occurs behind the trailing edge of low Reynolds number airfoils at low angles of attack prior to transition. The time-step was set to 0.01 convective turnovers. Further details regarding the numerical setup of the RANS simulations and the implementation of the  $\gamma - Re_\theta$  transition model can be found in [9]. For LES, the SD7003 geometry was extruded in the spanwise direction for 0.1 chords, which has been determined by [1] as sufficient for computing flow statistics at low and moderate angles of attack. The lateral boundaries were meshed conformally and assigned periodic boundary conditions. Several grids were tested to evaluate the influence of resolution on capturing small-scale structures, with the finest grid consisting of approximately 15 million cells. The grid ensures  $y_+$  values below 0.2 and  $x_+$  and  $z_+$  values below 5 near the airfoil. Furthermore, we verified that the grid resolves at least 80% of the turbulent kinetic energy in the spectrum. Simulations were performed using 128 cores of 4 Intel Xeon Scalable Processors Gold 6130 2.10 GHz. The time step employed in our simulation was 0.002 convective turnovers. The inner solver executed 10 iterations per time step, resulting in residuals dropping between 2 and 3 orders of magnitude. Simulations were conducted for 20 turnovers, and statistics were computed within the last 10. The Wall Adaptive Local Eddy-viscosity (WALE) sub-grid turbulence model and the Dynamic Smagorinsky approach were compared. The recommended spatial discretization in STAR-CCM+ is the second-order Bounded Central Difference (BCD) scheme. This scheme was compared with a third-order Central Difference (CD3) scheme, a third-order Monotonic Upwind Scheme for Conservation Laws (MUSCL3), and a hybrid scheme that combines third-order central difference and upwind schemes (CD/MUSCL3). Third-order schemes demonstrated no significant overhead compared to the bounded central difference scheme implemented in STAR-CCM+. Compared to the standard second-order upwind scheme, the overhead was approximately 10%. Despite these small overheads, the enhanced accuracy of third-order schemes, as demonstrated by Ricci et al. [11], could outweigh the additional computational costs.

## Results and Discussion

Figure 1 illustrates the Q-criterion iso-surface obtained using the CD3 scheme, revealing an artificial structure outside the boundary layer resulting from solver instability. Conversely, the hybrid CD/MUSCL3 scheme with a blending factor of 0.15 proved to be stable and robust. In Figure 2, the friction coefficient for our simulations is compared to the results presented by Galbraith & Visbal [1]. It is important to note that their simulations were conducted at a Mach number of 0.1. However, we believe this discrepancy is likely insufficient to account for the variations observed in Figure 2. Our simulations exhibit a delayed separation transition and reattachment, with separation bubbles of the same length but shifted toward the trailing edge. These differences indicate that dissipation remains a significant factor, necessitating further grid refinements to ensure that grid-related issues do not influence this phenomenon. Nevertheless, some intriguing observations can still be made. Firstly, reducing the blending factor clearly decreases dissipation, which is associated with an artificially rapid decay of turbulent kinetic energy when using upwind schemes. Additionally, we can observe that the Dynamic Smagorinsky approach demonstrates a higher level of turbulent kinetic energy production, anticipating the reattachment of the boundary layer.

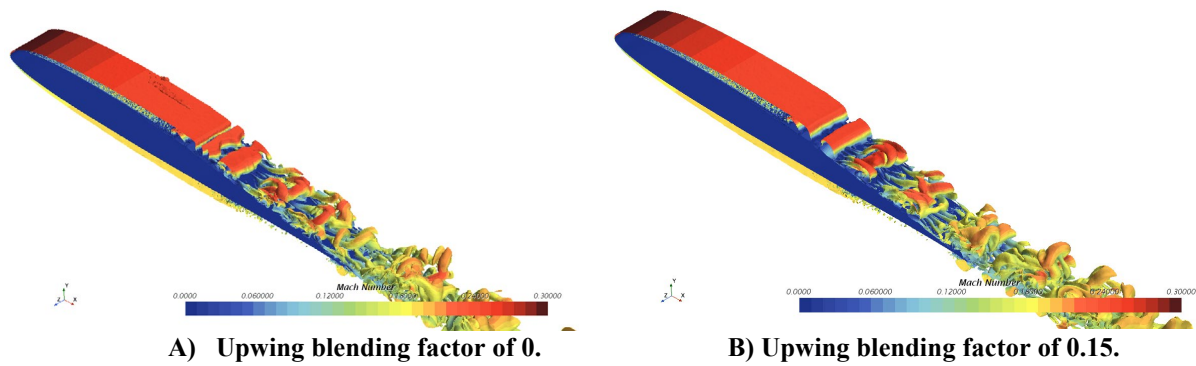


Figure 1.  $Q$ -criterion=500 Isosurface coloured with Mach number. CD3/MUSCL3 Scheme.

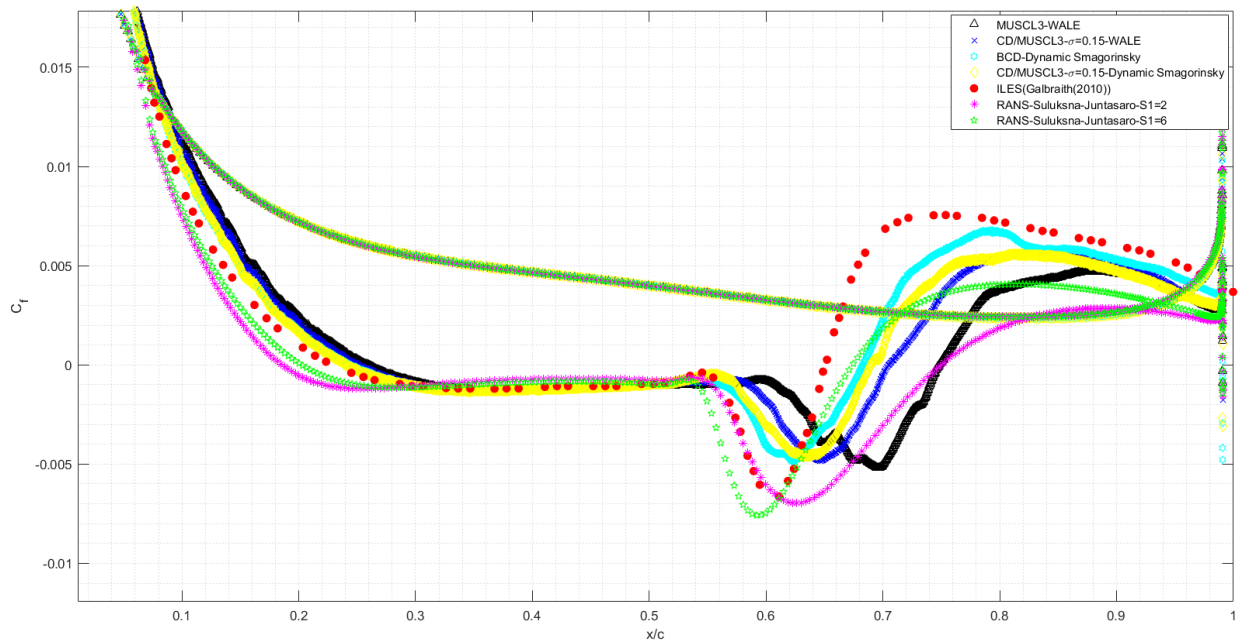


Figure 2. Time-averaged friction coefficient at the mid-span plane.

When comparing our RANS and LES approaches, we observe a noticeable shift of the separation bubble towards the trailing edge. This discrepancy arises because the RANS model follows the recalibration performed in reference [9], which utilized the Galbraith ILES results [1] as a reference. Nevertheless, the overall agreement is satisfactory. Figure 3 depicts the averaged velocity fields, revealing the presence of a separation bubble in both cases. Once again, we observe a slight shift of the bubble towards the trailing edge in the LES simulation. Notably, the LES simulation predicts a much sharper closure of the separation bubble, leading to a higher friction coefficient after reattachment. This discrepancy in skin friction under-prediction becomes more pronounced at lower Reynolds numbers [9] and is associated with excessive damping of turbulent kinetic energy production near the airfoil wall in the RANS model. Despite these discrepancies, Figure 3 highlights the usefulness of a well-tuned transition model, enabling accurate performance predictions with two-dimensional simulations that require a computational cost of approximately 1 CPU-hour, compared to around 40,000 CPU-hours for the 3D LES simulations. Furthermore, it opens up the possibility of enhancing the accuracy of RANS simulations in complex three-dimensional scenarios, such as flow over a rotor, where LES remains currently unaffordable.

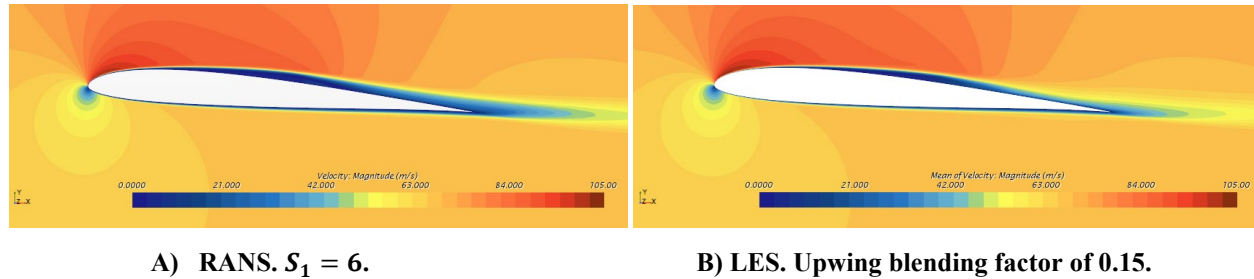


Figure 3. Time-averaged velocity magnitude fields at the mid-span plane.

## References

- [1] Galbraith, M., & Visbal, M, Implicit large eddy simulation of low-Reynolds-number transitional flow past the SD7003 airfoil. In 40th fluid dynamics conference and exhibit (2010) AIAA-4737. <https://doi.org/10.2514/6.2010-4737>
- [2] Uranga, A., Persson, P. O., Drela, M., & Peraire, J. Implicit large eddy simulation of transitional flows over airfoils and wings. In 19th AIAA Computational Fluid Dynamics (2009) AIAA- 4131. <https://doi.org/10.2514/6.2009-4131>
- [3] Catalano, P., & Tognaccini, R. Large eddy simulations of the flow around the SD7003 airfoil. In AIMETA Conference (2011) pp. 1-10.
- [4] Windte, J., Scholz, U., and Radespiel, R., “Validation of RANS Simulation of Laminar Separation Bubbles on Airfoils,” *Aerospace Science and Technology Journal*, Vol. 10, No. 7, 2006, pp. 484–494. <https://doi.org/10.1016/j.ast.2006.03.008>
- [5] Catalano, P. and Tognaccini, R., “Turbulence Modelling for Low Reynolds Number Flows,” *AIAA Journal*, Vol. 48, No. 8, 2010, pp. 1673–1685. <https://doi.org/10.2514/1.J050067>
- [6] Catalano, P. and Tognaccini, R., “RANS analysis of the low-Reynolds number flow around the SD7003 airfoil,” *Aerospace Science and Technology Journal*, 2011. <https://doi.org/10.1016/j.ast.2010.12.006>
- [7] De Santis, C., Catalano, P., & Tognaccini, R. (2022). Model for enhancing turbulent production in laminar separation bubbles. *AIAA Journal*, 60(1), 473-487. <https://doi.org/10.2514/1.J060883>
- [8] Menter, F. R., Smirnov, P. E., Liu, T., & Avancha, R. (2015). A one-equation local correlation-based transition model. *Flow, Turbulence and Combustion*, 95, 583-619. <https://doi.org/10.1007/s10494-015-9622-4>
- [9] Carreño Ruiz, M., D’Ambrosio, D. Validation of the  $\gamma$ -Re  $\theta$  Transition Model for Airfoils Operating in the Very Low Reynolds Number Regime. *Flow Turbulence Combust* 109, 279–308 (2022). <https://doi.org/10.1007/s10494-022-00331-z>
- [10] Langtry, R. B., & Menter, F. R. (2009). Correlation-based transition modeling for unstructured parallelized computational fluid dynamics codes. *AIAA journal*, 47(12), 2894-2906. <https://doi.org/10.2514/1.42362>
- [11] Ricci, F. & Strobel, P. & Tsoutsanis, P. & Antoniadis, A. Hovering rotor solutions by high-order methods on unstructured grids. *Aerospace Science and Technology*. (2019). <https://doi.org/10.1016/j.ast.2019.105648>